Synthesis, Base Pairing, and Fluorescence Properties of Oligonucleotides Containing 1*H*-Pyrazolo[3,4-*d*]pyrimidin-6-amine (8-Aza-7-deazapurin-2-amine) as an Analogue of Purin-2-amine

by **Frank Seela*** and **Georg Becher**

Laboratorium für Organische und Bioorganische Chemie, Institut für Chemie, Universität Osnabrück, Barbarastrasse 7, D-49069 Osnabrück

In memory of Prof. Dr. *Alexander Krayevsky*

The synthesis of the N^9- and N^8-(β-D-2′-deoxyribonucleosides) **2** and **10**, respectively, of 8-aza-7-deazapurin-2-amine (=1*H*-pyrazolo[3,4-*d*]pyrimidin-6-amine) is described. The fluorescence properties and the stability of the *N*-glycosylic bond of **2** were determined and compared with those of the 2′-deoxyribonucleosides **1** and **3** of purin-2-amine and 7-deazapurin-2-amine respectively. From the nucleoside **2**, the phosphoramidite **14** was prepared, and oligonucleotides were synthesized. Duplexes containing compound **1** or **2** are slightly less stable than those containing 2′-deoxyadenosine, while their CD spectra are rather different. The fluorescence of the nucleosides is strongly quenched (> 95%) in single-stranded as well as in duplex DNA. The residual fluorescence was used to determine the melting profiles, which gave T_m values similar to those determined from the UV melting curves.

Introduction. – Purin-2-amine preferentially pairs with thymine during DNA replication [1][2]. Bidentate base pairs are formed in oligonucleotides with parallel as well as antiparallel chain orientation [3]. Purin-2-amine is highly mutagenic. It causes dG-dC → dA-dT and dA-dT → dG-dC transitions [4][5]. The background for such transitions is due to base-pairing ambiguity. Purin-2-amine pairs with thymine and cytosine. Several motifs have been suggested for the purin-2-amine · cytosine base pair. The build-in fluorescence makes the purin-2-amine 2′-deoxyribonucleoside (**1**) [6] to a powerful structural and functional probe in nucleic acid chemistry and biology [7–12]. Several routes have been developed for the synthesis of the purin-2-amine ribo- and 2′-deoxyribonucleoside [13–16]. Oligonucleotides containing purin-2-amine have been prepared [17–19].

We now report the synthesis of the pyrazolo[3,4-*d*]pyrimidin-6-amine nucleoside **2**, which is an 8-aza-7-deazapurin-2-amine analogue of the purin-2-amine nucleoside **1**. Part of this work has been reported as an abstract and a short communication [21][22]. The nucleoside **2** is expected to show *Watson-Crick* base-pairing properties similar to those of **1** when it is incorporated in oligonucleotides. However, stacking interactions might be affected due to changes in the five-membered ring structure. Such an effect has already been observed in the case of oligonucleotides containing 8-aza-7-deaza-2′-deoxyadenosine (**4**) instead of the regular 2′-deoxyadenosine (**5**). As the purine nucleoside **1** and its pyrrolo[2,3-*d*]pyrimidine (= 7-deazapurine) derivative **3** are fluorescent [20], the same is expected for compound **2**.

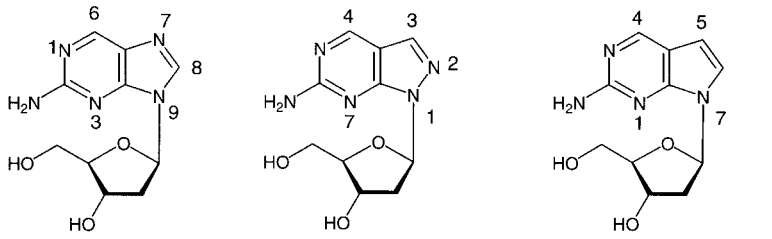

1
purine numbering

2
systematic numbering

3
systematic numbering

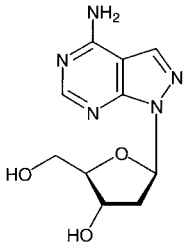

4

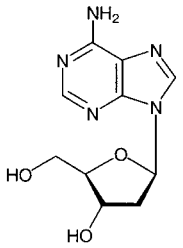

5

Results and Discussion. – *Synthesis of Monomers.* The synthesis of nucleoside **2** (purine numbering is used throughout the discussion section), uses 6-chloro-8-aza-7-deazapurin-2-amine (=4-chloro-1*H*-pyrazolo[3,4-*d*]pyrimidin-6-amine; **6**) [23] as precursor (*Scheme 1*). The glycosylation of **6** with 2-deoxy-3,5-di-*O*-(*p*-toluoyl)-*erythro*-pentofuranosyl chloride **7** was performed in a biphasic mixture of THF and 30% KOH solution instead of by the commonly used conditions (MeCN with powdered KOH and TDA-1 (=tris[2-(2-methoxyethoxy)ethyl]amine). This was necessary to overcome the low solubility of **6** in MeCN. The regioisomers **8** and **9** formed were separated by flash chromatography (FC) and isolated in about equal yields (40% of **8** and 39% of **9**). The position of the glycosylation was determined from the characteristic ^{13}C-NMR chemical shifts of the angular C-atoms (see below, *Table 1*) [24]. The β-D-configuration was assigned according to the ^{1}H-NMR chemical shift differences of H–C(4′) and 2 H–C(5′) of the toluoylated compounds **8** and **9** [25]. Subsequently, the regioisomeric nucleosides **8** and **9** were dehalogenated by catalytic hydrogenation, yielding protected intermediates, which were not isolated but directly deblocked with 0.5M NaOMe/MeOH to give the nucleosides **2** and **10**, respectively.

Compound **2** is rather stable at its *N*-glycosylic bond and is not hydrolyzed in 0.1N HCl at room temperature. The purin-2-amine nucleoside **1** is significantly less stable under these conditions (τ 170 min). The hydrolysis was followed UV-spectrophotometrically [24] as well as by HPLC analysis (260 nm). For the identification of the hydrolysis products, the 8-aza-7-deazapurin-2-amine (**11**) was prepared from com-

Scheme 1

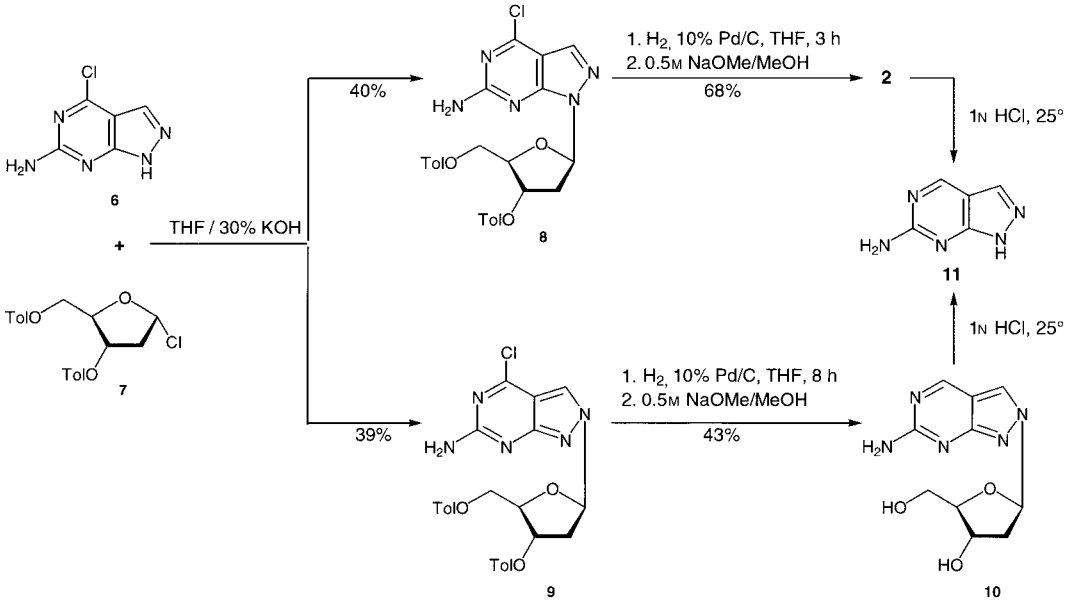

pound **6** by catalytic hydrogenation. The hydrolysis of the glycosylic bond of the N^8-nucleoside **10** (1N HCl at 25°) occurred much faster than in the case of the N^9-nucleoside **2** (τ 167 min for **2** and 5 min for **10**).

The UV spectra of the nucleosides **1** (304 nm) and **2** (305 nm) are nearly identical, while compound **3** shows a maximum at 311 nm. The maximum of the N^8-isomer **10** is bathochromically shifted (327 nm). The 8-aza-7-deazapurine nucleoside **2** exhibits a significant fluorescence with an emission maximum at 376 nm (excitation at 305 nm) (*Fig. 1,b*). The *Stokes* shift ($\Delta\lambda = 71$ nm) is larger than in the case of the purine nucleoside **1** ($\Delta\lambda = 59$ nm; excitation at 304 nm, emission at 363 nm) but smaller than that of the 7-deazapurine analogue **3** ($\Delta\lambda = 84$ nm) (*Fig. 1,c*). The N^8-nucleoside **10** shows an emission at 423 nm when excitated at 320 nm. The fluorescence spectra of the nucleosides were measured in H_2O at pH 7 at 10^{-5} M concentration. Next, the quantum yields for the nucleosides **1**–**3** were determined by two different methods, *i*) from the fluorescence life times and *ii*) by comparing the integrated areas of the emission curves of compound **1** and of the unknown samples **2** or **3**. The samples were excitated at a wavelength obtained from the UV curve intersection. Compound **1** with a quantum yield ϕ_f of 0.72 served as the standard. Comparison of the integrated fluorescence areas between **1** and the nucleosides **2** or **3** resulted in a quantum yield Φ_f of 0.53 for **2** and 0.47 for **3**. Nevertheless, compared to canonical nucleosides, a quantum yield of *ca.* 0.5 is still remarkably high, particularly when this behavior is present together with other favorable physical properties such as higher glycosylic bond stability or emission maxima shifted beyond the wavelengths of the parent nucleoside **1**.

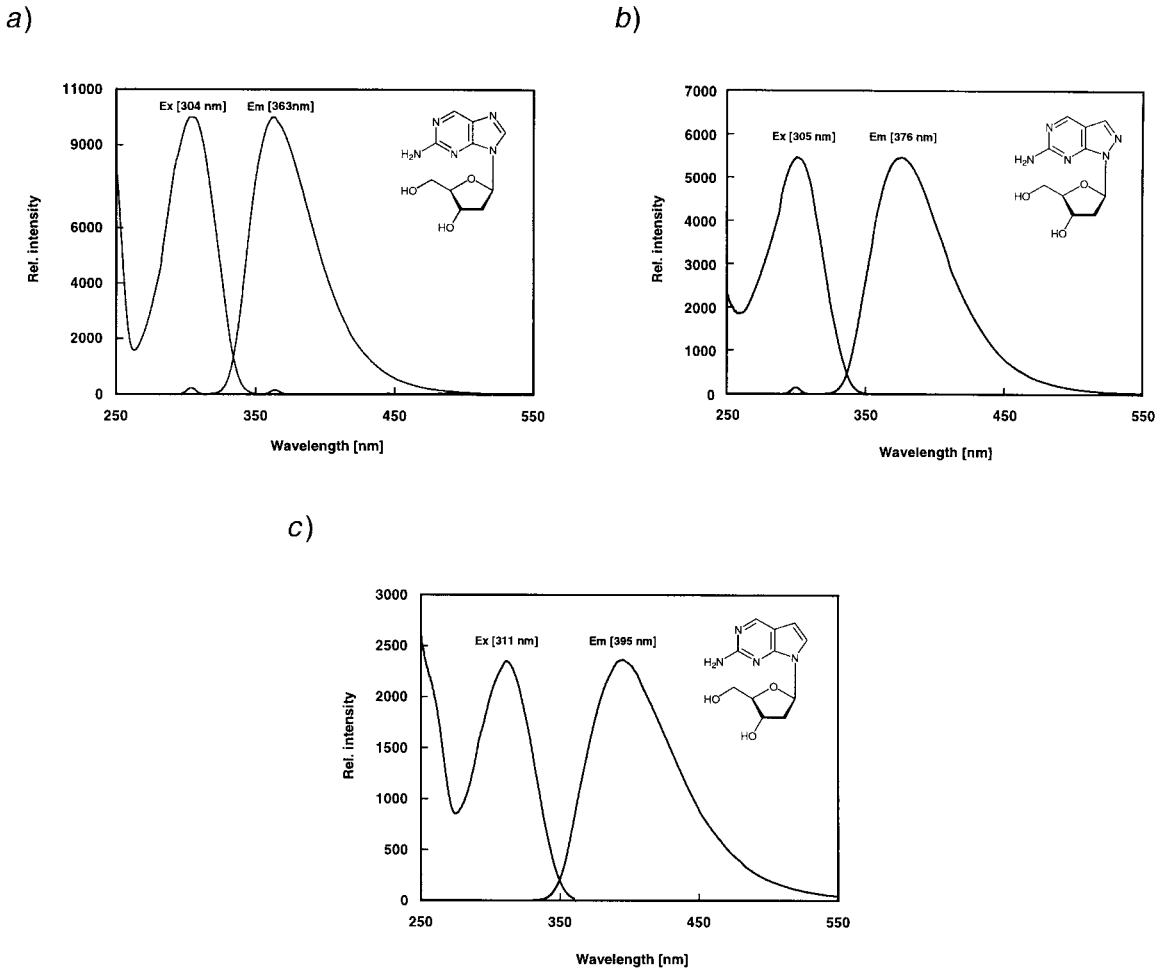

Fig. 1. *Fluorescence spectra of* a) *purin-2-amine 2′-deoxyribonucleoside* (**1**), b) *8-aza-7-deazapurin-2-amine 2′-deoxyribonucleoside* (**2**) *and* c) *7-deazapurin-2-amine 2′-deoxyribonucleoside* (**3**). Measured in double-distilled H_2O at 10^{-5} M concentration.

Next, the 2-amino function of **2** was blocked with a (dimethylamino)methylidene residue and with an acyl protecting group (*Scheme 2*). The amidine derivative **12a** was prepared under the usual reaction conditions in DMF solution [26][27]. For the phenoxyacetyl (pac) derivative **12b**, the protocol of transient protection was used [28], with a preceding conversion of the phenoxyacetyl chloride to the 2,4,5-trichlorophenyl phenoxyacetate derivative [29]. Formation of the protected nucleosides **12a**,**b** was verified by the ^{1}H- and ^{13}C-NMR spectra. The stability of the protecting group was determined by UV spectrophotometry in 25% ammonia (40°) at 310 nm for the formamidine-protected nucleoside **12a** and at 290 nm for the acyl derivative **12b**. The half-life was 60 min for **12a** and 1.5 min for **12b**.

Scheme 2

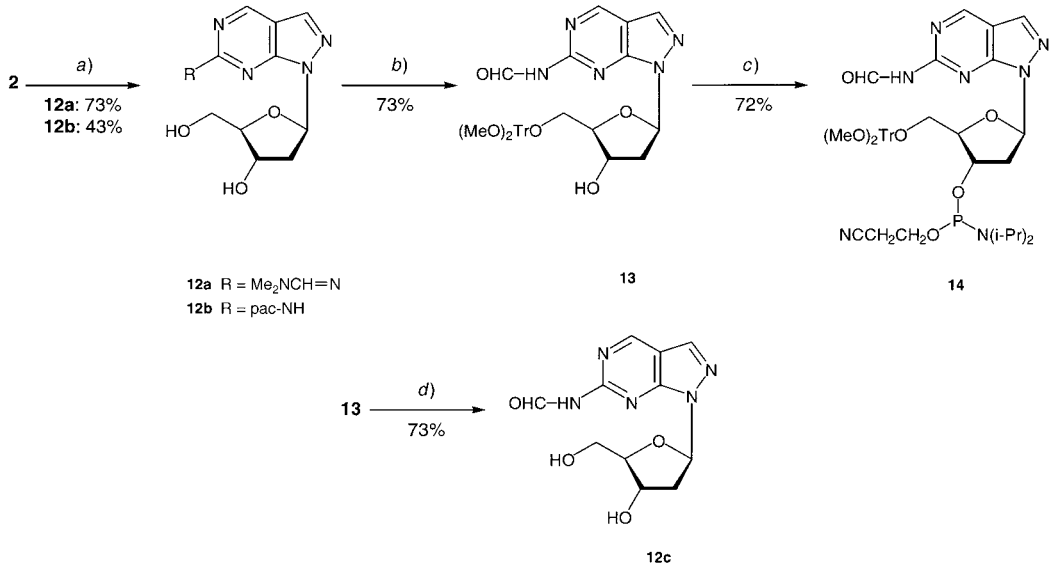

a) **12a**: DMF/dimethylformamide dimethyl acetal, r.t., 2 h; **12b**: pyridine, Me_3SiCl, 2,4,5-trichlorophenyl phenoxyacetate, 40°, 12 h. *b*) Pyridine/$(MeO)_2Tr-Cl$, r.t., 4 h. *c*) THF, 2-cyanoethyl diisopropylphosphoramidochloridite, r.t., 30 min. *d*) $CHCl_2COOH$, CH_2Cl_2, r.t., 5 min.

Subsequently, the protected intermediate **12a** was tritylated with 4,4′-dimethoxytrityl ($(MeO)_2Tr$) chloride by the standard protocol [30]. Instead of the amidine derivative, the formyl compound **13** was isolated (73%). A similar reaction was already reported for the 5-aza-7-deaza-2′-deoxyguanosine [31] and also for the 8-aza-7-deaza-2′-deoxyadenosin-2-amine [32]. Nevertheless, the formyl derivative **13** was stable enough for further manipulations, as the detritylation (Cl_3CCOOH/CH_2Cl_2) was not accompanied by a deformylation of the rather labile derivative **12c** (τ 3 min). Finally, the phosphoramidite **14** was prepared [33].

All compounds were characterized by ^1H-, ^{13}C-, and ^{31}P-NMR spectroscopy and by elemental analysis (*Tables 1* and *2* and *Exper. Part*). For the assignment of the ^{13}C-NMR chemical shifts, gated-decoupled spectra were measured (see *Table 2*). In the gated-decoupled spectrum of compound **8** with the Cl-substituent at C(4), 2*s* for C(4) at 155.2 ppm and for C(6) at 161.0 ppm are found. Compound **2** shows 2*d* for C(4) ($^1J = 186$ Hz) and a long-range coupling of $^4J = 12$ Hz for C(3). The determination of C(1′) and C(4′) is based on the observation that the coupling constant ^1J(C,H) of C(1′) is larger than that of C(4′) [34].

2. *Oligonucleotides.* 2.1. *Synthesis and Characterization*. Oligonucleotide synthesis was performed on solid phase by the standard protocol; the coupling efficiency of **2** was always higher than 95%. The oligonucleotides were detritylated and purified on purification cartridges. The homogeneity of the oligonucleotides **15**–**30** (see *Tables 3* and *4*) was established by ion-exchange chromatography on a 4 × 25-cm *NucleoPac-PA-100* column (*Dionex*; P/N 043018, USA) and their composition determined by tandem hydrolysis with snake-venom phosphodiesterase and alkaline phosphatase as

Table 1. *^{13}C-NMR Chemical Shifts of 8-Aza-7-deazapurine* (= 1*H*-Pyrazolo[3,4-*d*]pyrimidine) *2′-Deoxyribonucleosides*[a])

	C(7)[b]) C(3)[c])	C(5)[b]) C(3a)[c])	C(6)[b]) C(4)[c])	C(2)[b]) C(6)[c])	C(4)[b]) C(7a)[c])	CH	C=O	MeO	C(1′)	C(2′)	C(3′)	C(4′)	C(5′)
2	134.3	107.9	154.2	162.0	155.4				82.8	37.7	71.1	87.4	62.5
6 [23]	132.5	105.7	153.1	161.4	157.4								
8	133.6	108.7	155.2	161.0	156.6				85.0	35.6	75.5	82.4	64.2
9	123.6	108.2	157.3	160.4	161.7				91.6	38.8	74.9	84.2	60.3
10	125.5	106.9	157.3	161.1	160.4				90.4	40.5	70.5	88.4	61.9
11	133.6	107.0	153.6	162.0	156.3								
12a	134.3	110.5	153.7	158.9	155.3	158.7			83.3	37.9	71.1	87.6	62.6
b	134.8	111.4	153.7	155.2	154.8		166.0		83.6	37.8	71.1	87.8	62.4
c	134.8	112.0	153.5	155.6	154.8		163.5		83.4	37.7	71.0	87.6	62.3
13	134.8	112.2	153.5	155.7	154.9		163.6	55.0	83.6	38.2	70.7	85.6	64.3

[a]) Measured in (D_6)DMSO at 298 K. [b]) Purine numbering. [c]) Systematic numbering.

Table 2. *Coupling Constants J(C,H)* [Hz] *of 8-Aza-7-deazapurine* (= 1*H*-Pyrazolo[3,4-*d*]pyrimidine) *2′-Deoxyribonucleosides*[a])[b])

	2	**8**	**12a**		**2**	**8**	**12a**
J(6, H–C(4))	12	–	8	*J*(1′, H–C(1′))	163	166	158
J(3a, H–C(4))	11	–	9	*J*(3′, H–C(3′))	147	158	148
J(3a, H–C(3))	11	11	9	*J*(4′, H–C(4′))	148	152	140
J(4, H–C(4))	186	–	178	*J*(5′, H–C(5′))	140	149	140
				J(CH=N, C*H*=N)	–	–	202

[a]) Conditions, see *Table 1*. [b]) Systematic numbering.

described [35]. An example of a digestion pattern and a MALDI-TOF spectrum is shown in *Fig. 2* (see *Exper. Part* for MALDI-TOF data).

2.2. *Duplex Stability.* At first, compound **2** was introduced into the self-complementary duplex 5′-d[(GTA**GAATTC**TAC)]$_2$ (**15**·**15**), which contains the recognition site of the endodeoxyribonuclease Eco RI (boldface). Replacement of all four dA residues by compound **2** reduced the T_m value by 10° (see **16**·**16** in *Table 3*). This amounts to a T_m decrease of 1.2° per base modification. Similar results have been reported for the destabilization of the purin-2-amine 2′-deoxyribonucleoside **1** [16][17][36][37]. When the dA isostere **4** ($c^7z^8A_d$) was incorporated at the same positions, the T_m value was increased by 1° [35].

Next, the duplex stability of non-self-complementary duplexes were investigated. The duplex 5′-d(TAGGTCAATACT) (**18**) and 3′-d(ATCCAGTTATGA) (**19**) was used for such purposes as our laboratory standards. Similarly to the self-complementary duplex, a destabilization was observed for the duplex **18**·**19** when compound **2** replaced dA (see *Table 3*). The substitution of the canonical adenine base in one strand by four 8-aza-7-deazapurin-2-amine residues led to a T_m decrease of 5°, which is again a T_m drop of *ca.* 1° per modified residue (see **20**·**19**). Surprisingly, no further T_m decrease was observed when also the second strand was modified (see **20**·**21**). The CD spectra in *Fig. 4*,*a* (see below) suggest a reasonable explanation for this phenomenon. With an

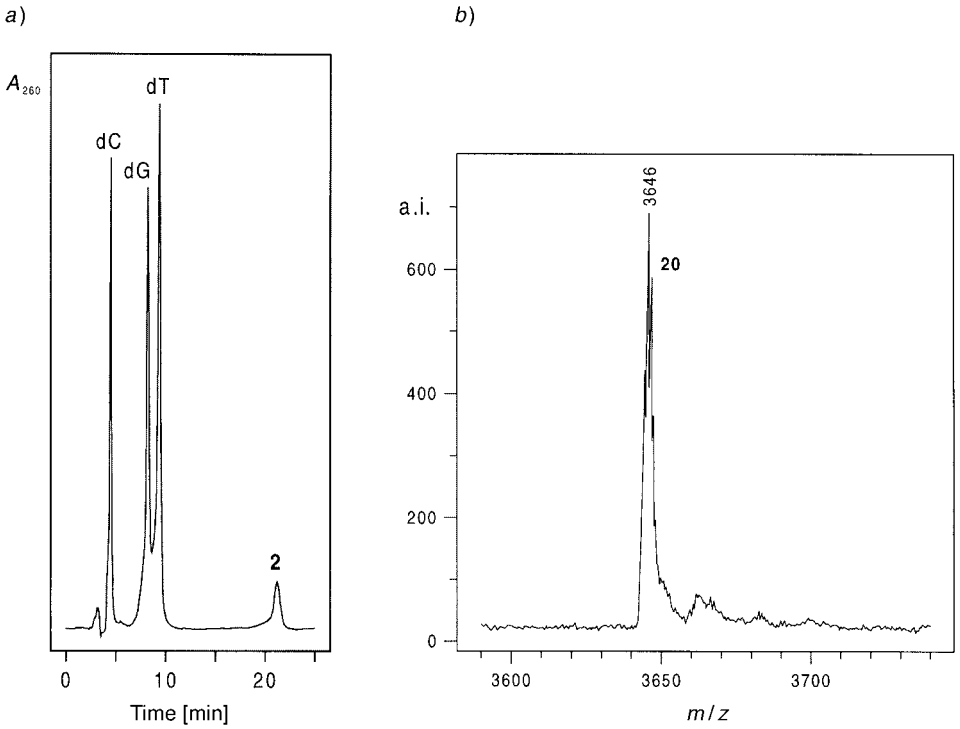

Fig. 2. a) *HPLC Profile of the reaction products obtained after enzymatic hydrolysis of the oligomer* **20** *with snake-venom phosphodiesterase and alkaline phosphatase in* 1M Tris · *HCl buffer* (pH 8.0) *at 37°* (column: *RP-18* (200 × 10 mm); gradient: 0–30 min in 0.1M (Et_3NH)OAc (pH 7.0)/MeCN 95:5). b) *MALDI-TOF Mass spectrum of oligomer* **20** *measured on a* Biflex-III *instrument.*

increasing number of modifications, the helical structure changes from the typically B-DNA type to a different DNA type. The incorporation of the parent purin-2-amine 2′-deoxyribonucleoside (**1**) resulted in a similar T_m decrease when it replaced **2** (see **22** · **19** in *Table 3*). Furthermore, when the number of replacements of the adenine base by purin-2-amine was high (see **22** · **23**), only a linear increase of the UV absorption was observed, as it was described before for other duplexes [36][41]. Nevertheless, the incorporation of 8-aza-7-deazapurin-2-amine at the same position still gave a sigmoidal melting profile (*e.g.*, **20** · **21**).

It is well-documented that the ambiguous base pairing of compound **1** with dT as well as with dC causes mutagenicity [4][5]. Earlier, several base pairs of compound **1** with dC have been suggested [2][38]. From recent work [39], the wobble pair **III** represents the most likely structure for the base pair of compound **1** with dC. The same pairing mode is now anticipated for compound **2** (see **IV**). When compound **2** forms a base pair with dC, the duplex is more labile than the *Watson-Crick* base pair **I** of compound **2** with dT. This was demonstrated in the case of the duplex **28** · **21** (T_m 34°) as compared to the duplex **20** · **21** (T_m 42°). A similar T_m decrease was observed when compound **1** was used instead of **2** (see **28** · **23**, T_m 32°).

Table 3. T_m *Values and Thermodynamic Data of Oligonucleotides with Antiparallel Chain Orientation*[a])

	T_m [°C][a])	ΔH^0 [kcal/mol]	ΔS^0 [cal/mol·K]	ΔG_{298} [kcal/mol]
5′-d[(GTAGAATTCTAC)]$_2$ [35] (**15**·**15**)	43	– 84	– 225	– 8.6
5′-d[(GT**2**G**22**TTCT**2**C)]$_2$ (**16**·**16**)	33	– 59	– 169	– 6.5
5′-d[(GT**4**G**44**TTCT**4**C)]$_2$ [35] (**17**·**17**)	44	– 65	– 183	– 8.7
5′-d(TAG GTC AAT ACT) (**18**·**19**) 3′-d(ATC CAG TTA TGA)	46	– 86	– 230	– 10.3
5′-d(T**2**G GTC **22**T **2**CT) (**20**·**21**) 3′-d(ATC C**2**G TT**2** TG**2**)	42	– 91	– 261	– 9.4
5′d(T**1**G GTC **11**T **1**CT) (**22**·**23**) 3′-d(ATC C**1**G TT**1** TG**1**)	[b])	–	–	–
5′-d(T**4**G GTC **44**T **4**CT) [35] (**24**·**25**) 3′-d(ATC C**4**G TT**4** TGA)	47	– 97	– 260	– 10.9
5′-d(T**2**G GTC **22**T **2**CT) (**20**·**19**) 3′-d(ATC CAG TTA TGA)	41	– 81	– 232	– 9.2
5′-d(T**1**G GTC **11**T **1**CT) (**22**·**19**) 3′-d(ATC CAG TTA TGA)	40	– 59	– 160	– 8.6
5′-d(TAG GTC AAT ACT) (**18**·**21**) 3′-d(ATC C**2**G TT**2** TG**2**)	42	– 81	– 229	– 9.5
5′-d(TAG GTC AAT ACT) (**18**·**23**) 3′-d(ATC C**1**G TT**1** TG**1**)	42	– 92	– 265	– 9.8
5′-d(T**2**G GTC AAT ACT) (**26**·**19**) 3′-d(ATC CAG TTA TGA)	46	– 84	– 237	– 10.2
5′d(TAG GTC **22**T ACT) (**27**·**19**) 3′-d(ATC CAG TTA TGA)	43	– 81	– 233	– 9.3
5′-d(TAG G**C**C AA**C** ACT) (**28**·**21**) 3′-d(ATC C**2**G TT**2** TG**2**)	34	– 68	– 195	– 7.2
5′-d(TAG G**C**C AA**C** ACT) (**28**·**23**) 3′-d(ATC C**1**G TT**1** TG**1**)	32	– 76	– 222	– 6.8

[a]) Measured in 0.1M NaCl, 100 mM $MgCl_2$ and 10 mM Na-cacodylate buffer, pH = 7.0 at 260 nm. Single strand concentration is 5 μM. Numbers refer to the related nucleosides. [b]) Only linear increase of the UV absorption.

Finally, the stability of duplexes with parallel strand (ps) orientation was investigated. For this purpose, it was necessary to exchange the dG·dC pair with an $iG_d \cdot C_d$ and/or $dG \cdot m^5iC_d$ pair. As standard duplexes, the hybrids **29**·**18** and **30**·**19** were chosen [40], and several dA·dT base pairs were replaced by base pairs formed by compound **2** and dT (see *Table 4*). As already shown in the case of aps-duplexes (aps = antiparallel strand), the duplex stability of ps-duplexes was reduced when the nucleoside **2** was replacing dA (see T_m of **29**·**20** and **30**·**21** in *Table 4*). The decrease of the free energy was more pronounced in ps-DNA (3 kcal/mol) than in aps-DNA (1 kcal/mol), as shown by a comparison of the data of duplexes **19**·**20** and **18**·**21** (*Table 3*) with those of **29**·**20** and **30**·**21** (*Table 4*). The base-pairing mode of nucleoside **2** with dT is expected to occur *via* the base pair **II**.

Although the effects of compound **2** on the base-pair stability with dT or dC were similar to those of the nucleoside **1**, it was of interest to study the duplexes by CD spectroscopy. At first, the CD spectra of the nucleosides **1** and **2** were measured in 0.1M NaCl, 0.01M $MgCl_2$, and 10 mM Na-cacodylate buffer at pH 7.0. These CD spectra are quite different (*Fig. 3*,*a*) while the UV spectra are very similar (UV (MeOH): 304 nm

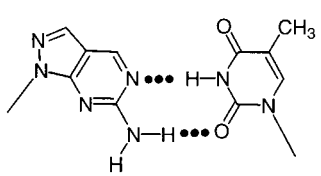

(aps) - *Watson Crick* base pair **I**

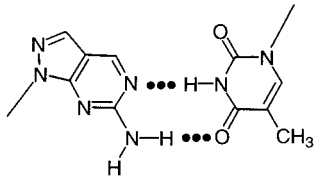

(ps) - reverse-*Watson Crick* base pair **II**

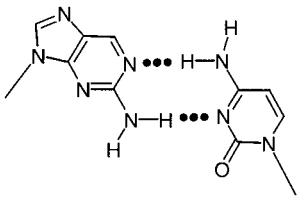

wobble base pair **III**

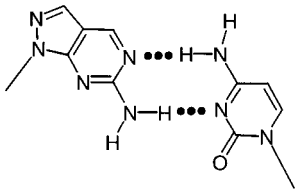

wobble base pair **IV**

Table 4. T_m *Values and Thermodynamic Data of Oligonucleotides with Parallel Chain Orientation*[a])

	T_m [°C]	ΔH^0 [kcal/mol]	ΔS^0 [cal/mol · K]	ΔG_{298} [kcal/mol]
5′-d(ATiC iCAiG TTA TiGA) (**29**·**18**) [40] 5′-d(TAG GTC AAT ACT)	39	– 74	– 211	– 8.8
5′-d(ATiC iCAiG TTA TiGA)[b]) (**29**·**20**) 5′-d(T**2**G GTC **22**T **2**CT)	25	– 52	– 176	– 5.9
5′-d(TiCA TAA iCTiG iGAT) (**30**·**19**) [40] 5′-d(AGT ATT GAC CTA)	44	– 85	– 242	– 10.3
5′-d(TiCA TAA iCTiG iGAT) (**30**·**21**) 5′-d(**2**GT **2**TT G**2**C CTA)	27	– 64	– 195	– 6.9

[a]) UV Measurements (260 nm) were performed in 1M NaCl, 0.1M $MgCl_2$, and 60 mM Na-cacodylate buffer, pH 7.0. Single strand concentration was 5 μM. [b]) $d(iC) = m^5iC_d$.

(5500) for **1** and 305 nm (5900) for **2**). The difference results from the special high-*anti*-conformation of the 8-aza-7-deazapurine nucleosides, which has been established by NMR spectroscopy as well as by single-crystal X-ray analysis [41].

Next, the CD spectra of the self-complementary duplexes **15**·**15**, **16**·**16**, and **17**·**17** were measured under the same conditions. *Fig. 3,b* indicates that the substitution of all eight adenine residues in **15**·**15** by 8-aza-7-deazapurin-2-amine (**2**) changes the CD spectrum significantly (see **16**·**16**), while the CD spectrum of the duplex **17**·**17** containing eight 8-aza-7-deazapurin-6-amine nucleosides (**4**) has still the shape of a spectrum of a B-DNA. According to that, the normal B-DNA changes into another DNA structure when a sufficient number of 8-aza-7-deazapurine nucleosides are present. Similar experiments as performed with the self-complementary duplexes **15**–**17** were performed with the non-self-complementary hybrids **18**·**19**, **20**·**21**, **22**·**23**, and

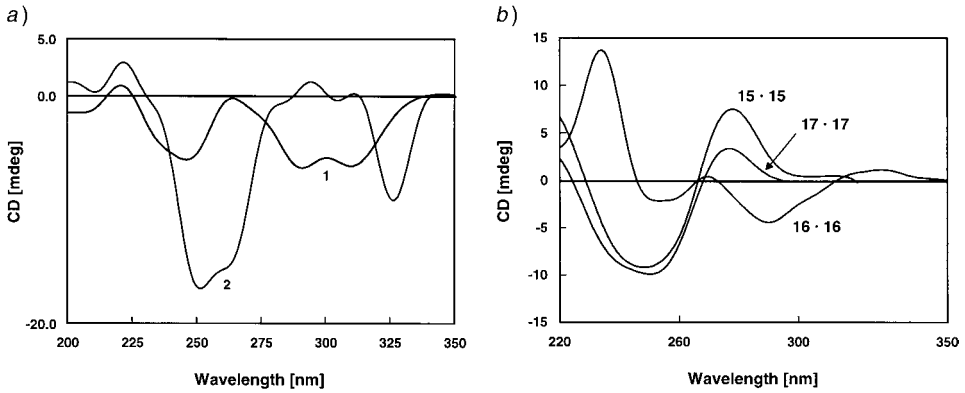

Fig. 3. a) *CD Spectra of the nucleosides* **1** *and* **2** *and* b) *CD spectra of the self-complementary duplexes* **15** · **15**, **16** · **16**, *and* **17** · **17**. Measured at 20° in 0.1M NaCl containing 10 mM $MgCl_2$ and 10 mM Na-cacodylate at pH 7.0.

24 · **25**. The structure of the DNA formed by **2** depends on the number of incorporated nucleosides (see *Fig. 4*,*a*). When only two nucleosides **2** were introduced, the shape of a B-DNA was still retained (see **27** · **19**). An increasing number of 8-aza-7-deazapurine nucleosides **2** – from four to seven modifications – changed the shape of the CD spectrum completely, indicating an overall change of the B-DNA structure (see **20** · **19** and **20** · **21**). Such strong changes were not observed when the duplex contained the purin-2-amine nucleoside **1** at the same seven positions (see **22** · **23** in *Fig. 4*,*b*; *cf.* also **24** · **25** containing six nucleoside units **4**).

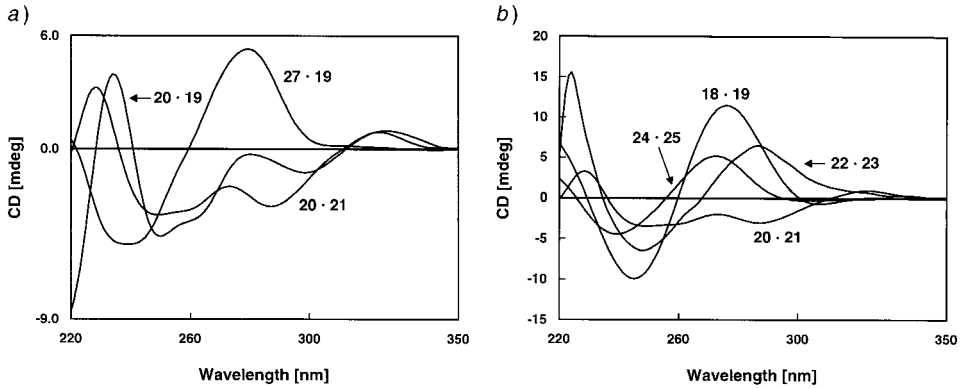

Fig. 4. a) *CD Spectra of the heteroduplexes* **27** · **19**, **20** · **19**, *and* **20** · **21** *with an increasing number of nucleoside* **2**; b) *CD spectra of the heteroduplexes* **18** · **19**, **20** · **21**, **22** · **23**, *and* **24** · **25**. For conditions, see *Fig. 3*,*a*.

2.3. *Fluorescence Properties.* Next, the fluorescence properties of the oligomers **20**, **22**, and **27** were analyzed. At first, the single-stranded oligomers **20** and **22** were hydrolyzed with snake-venom phosphodiesterase, and the fluorescence was measured before and after 12 h of cleavage (*Fig. 5*). The samples were subjected to excitation at 304 nm, and the emission was measured. Both nucleosides **1** and **2** show only a residual fluorescence intensity of less than 5% when they are incorporated in oligonucleotides.

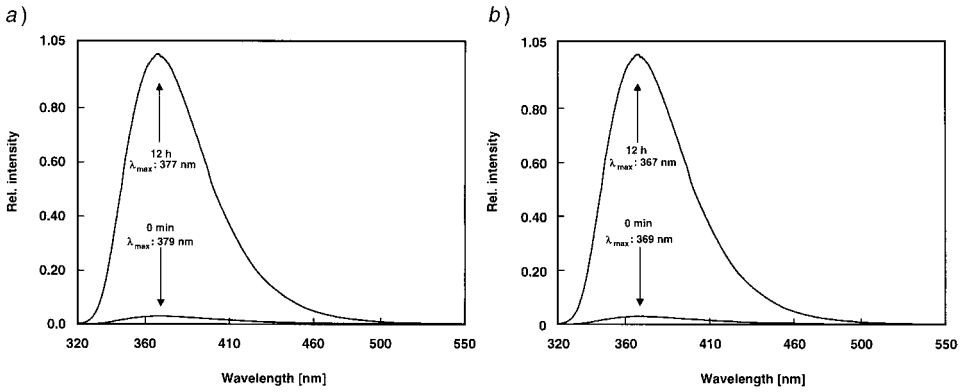

Fig. 5. *Emission spectrum of* a) **20** *and* b) **22** *before and after treatment with phosphodiesterase.* Measured in 0.1M *Tris* · HCl buffer (pH 8.0) at 20°; excitation wavelength 304 nm.

The emission maxima of the monomeric molecules are bathochromically shifted when they are incorporated in oligonucleotides.

To explain these observations, it should be remembered that DNA molecules – already in the single-stranded state – are strongly stacked. This is even true for dimers. A *ca.* 95% quenching is observed in the case of the dinucleoside monophosphate Gp**3** [20]. The decrease of fluorescence of compounds **1** or **2** incorporated into an oligonucleotide is a direct result of this 'static' stacking. The stacked compounds **1** or **2** are significantly less fluorescent than the free nucleosides. This results from the molecular surrounding of the molecules. A stacked helix provides many more quenching candidates than the free nucleosides surrounded by H_2O molecules.

In a second set of experiments, the fluorescence of the single-stranded oligomers **20** and **27** was measured at different temperatures (see *Fig. 6*). This shows a temperature-dependent decrease of the fluorescence due to increased collisional quenching; the static quenching induced by stacking interactions should be reduced with an increase in the temperature [42].

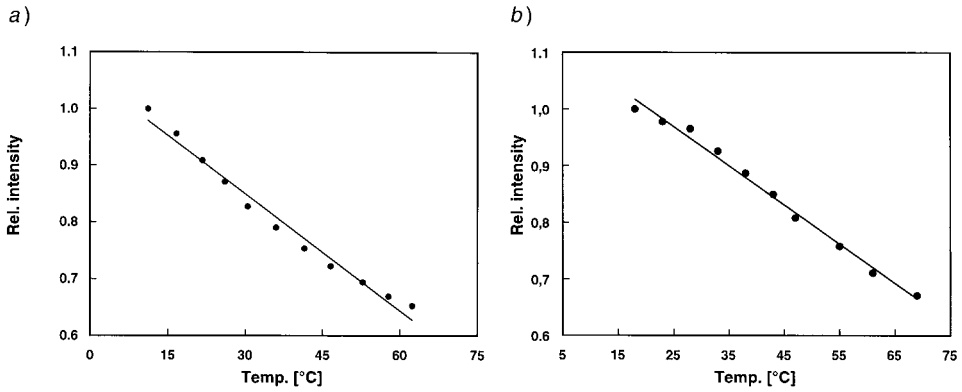

Fig. 6. *Temperature-dependent measurement of the fluorescence of* a) *the single strand* **27** *and* b) *the single strand* **20**. In 0.1M NaCl, 10 mM $MgCl_2$, and 10 mM Na-cacodylate at pH 7.0, with 0.4 A_{260} units.

In a third set of experiments, both single strands **20** and **27** were hybridized with the complementary unmodified oligomer **19**, with double the concentration of the unmodified strands to ensure complete hybridization at room temperature [43]. When the temperature was increased, a sigmoidal melting profile was observed, leading to a T_m value rather similar to that determined by UV measurements (*Fig. 7*) [42]. The decrease of the fluorescence at the end of the melting process resulted again from the collision with solvent molecules, as was already observed in the case of single-strand oligonucleotides. The same was observed for the duplex **22**·**19**, which contains four compound **1** residues. Differences in T_m values determined by UV or fluorescence measurements have been reported for self-complementary duplexes [42].

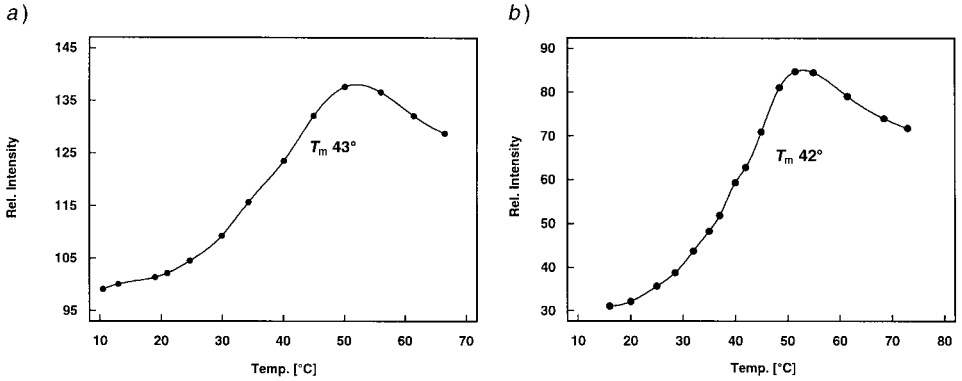

Fig. 7. *Temperature-dependent measurement of the fluorescence of* a) *the duplex* **27**·**19** *and* b) **20**·**19**. In 0.1M NaCl, 10 mM $MgCl_2$, and 10 mM Na-cacodylate at pH 7.0, with double the concentration of the oligomers **18** or **19** (0.8 A_{260} units).

We thank Dr. *H. Rosemeyer* and Mr. *Y. He* for the measurements of the NMR spectra. We also appreciate the measurements of the MALDI-TOF spectra by Dr. *T. Wenzel* (*Bruker*, Leipzig, Germany) and the determination of quantum yields obtained from the fluorescence life times by Dr. *M. Sauer*, Universität Heidelberg. Compounds **2**, **5**, and **8**–**10** have been described in the Thesis of Dr. *H. Steker*, Paderborn, Germany. Financial support by the *Deutsche Forschungsgemeinschaft* is gratefully acknowledged.

Experimental Part

General. See [35]. Purin-2-amine (2-cyanoethyl phosphoramidite) was obtained from *Eurogentec*, Belgium. Flash chromatography (FC): at 0.4 bar on *silica gel 60 H* (*Merck*, Darmstadt, Germany). Thin-layer chromatography (TLC): Aluminum sheets silica gel *60* F_{254} (0.2 mm, *Merck*, Germany). TLC Scanning: *CS-930* TLC scanner (*Shimadzu*, Japan). Solvent systems for FC and TLC: cyclohexane/AcOEt 4:1 (*A*), cyclohexane/AcOEt 3:2 (*B*), cyclohexane/AcOEt 1:4 (*C*), CH_2Cl_2/MeOH 95:5 (*D*), CH_2Cl_2/MeOH 9:1 (*E*), CH_2Cl_2/acetone 9:1 (*F*), CH_2Cl_2/AcOEt 90:10 (*G*), $CHCl_3$/MeOH 8:2 (*H*). M.p.: *Büchi-SMP-20 apparatus (Büchi*, Switzerland); not corrected. CD Spectra: *Jasco-600* (*Jasco*, Japan) spectropolarimeter with thermostatically (*Lauda-RCS-6* bath) controlled 1-cm cuvettes. UV Spectra: *150-20* spectrophotometer (*Hitachi*, Japan). Fluorescence spectroscopy: *F-4500* (*Hitachi*, Japan). NMR Spectra: *AC-250* and *AMX-500* spectrometers (*Bruker*, Germany); δ values in ppm downfield from internal $SiMe_4$ (^1H, ^{13}C). MALDI-TOF MS were measured by Dr. *T. Wenzel* (*Bruker*) with a *Biflex-III* instrument (see *Table 5*). Microanalyses were performed by *Mikroanalytisches Labor Beller* (Göttingen, Germany).

Oligonucleotides. Oligonucleotide synthesis was performed on a *ABI-392-DNA* synthesizer (*Applied Biosystems*, Weiterstadt, Germany) according to the standard protocol in the 'trityl-on' mode. The coupling

Table 5. M^+ *Data of Oligonucleotides Determined by MALDI-TOF Mass Spectrometry*

	M^+ (calc.)	M^+ (found)
5′-d(GT**2** G**22** TTC T**2**C) (**16**)	3644	3646
5′-d(TAG GTC AAT ACT) (**18**)	3644	3645
5′-d(AGT ATT GAC CTA) (**19**)	3644	3645
5′-d(T**2**G GTC **22**T **2**CT) (**20**)	3644	3646
5′-d(**2**GT **2**TT G**2**C CTA) (**21**)	3644	3644
5′-d(T**2**G GTC AAT ACT) (**26**)	3644	3646
5′-d(TAG GTC **22**T ACT) (**27**)	3644	3646

yields of modified phosphoramidites were on average 95% (trityl-conductivity monitoring). The oligomers were purified with oligonucleotide-purification (OP) cartridges (*Applied Biosystems*, Weiterstadt, Germany) by the standard protocol. The oligonucleotides were lyophilized on a *Speed-vac* evaporator to yield colorless solids, which were dissolved in 100 µl of double-distilled H_2O, and the purity of the oligomers were controlled by ion-exchange chromatography on a *Dionex-Nucleopac-PA-100* HPLC column (4 × 250 mm, P/N 043010; *Dionex*, Idstein, Germany). Melting curves were measured with a *Cary-1/3*-UV/VIS spectrophotometer (Varian, Australia) equipped with a Cary thermoelectrical controller. The actual temp. was measured in the reference cell with a Pt-100 resistor. The enzymatic hydrolysis of the oligomers was performed as described [35] using the following extinction coefficients: ε_{260}: ^7G_d 2700, dT 8800, dC 7300, dA 15400, dG 11700. Snake-venom phosphodiesterase (EC 3.1.15.1, *Crotallus durissus*) and alkaline phosphatase (EC 3.1.3.1, *E. coli*) were generous gifts from *Roche Diagnostics GmbH*.

*1*H-*Pyrazolo[3,4-*d*]pyrimidin-6-amine* (**11**). To 4-chloro-1*H*-pyrazolo[3,4-*d*]pyrimidin-6-amine (**6**; 4 g, 23.6 mmol) [23] in THF/MeOH 1:1 (250 ml), 10% Pd/C (2.5 g) was added and the mixture hydrogenated for 6 h at r.t. The catalyst was filtered and washed with hot MeOH (3×). The combined filtrate was evaporated, the residue dissolved in MeOH, and the soln. adsorbed onto silica gel (10 g) and submitted to FC (column 10 × 5 cm, *H*): **11** (1.65 g, 52%). Colorless needles. M.p. 272–274°. TLC (*H*): R_f 0.7. UV (MeOH): 224 (25100), 303 (6000). ^{1}H-NMR ((D$_6$)DMSO): 6.74 (*s*, NH_2); 7.91 (*s*, H–C(3)); 8.77 (*s*, H–C(4)); 12.93 (*s*, NH). Anal. calc. for $C_5H_5N_5$ (135.13): C 44.44, H 3.73, N 51.83; found: C 44.67, H 3.77, N 51.85.

*4-Chloro-1-[2-deoxy-3,5-di-*O*-(*p*-toluoyl)-β-*D*-*erythro*-pentofuranosyl]-1*H*-pyrazolo[3,4-*d*]pyrimidin-6-amine* (**8**) *and 4-Chloro-2-[2-deoxy-3,5-di-*O*-(*p*-toluoyl)-β-*D*-erythro-pentofuranosyl]-1*H*-pyrazolo[3,4-*d*]pyrimidin-6-amine* (**9**). By gentle warming, **6** (600 mg, 3.5 mmol) was dissolved in 30% aq. KOH soln. (4 ml). The soln. was cooled to r.t. and covered with a soln. of 2-deoxy-3,5-di-*O*-(*p*-toluoyl)-β-*D*-*erythro*-pentofuranosyl chloride (**7**; 1.8 g, 4.6 mmol) in THF. The layers were vigorously mixed for 2 min. Thereupon, CH_2Cl_2 (70 ml) was added, the org. layer dried (Na_2SO_4) and evaporated, and the yellowish oily residue dissolved in CH_2Cl_2 and chromatographed (silica gel, column 15 × 5 cm, $A \rightarrow C$). From the fast migrating zone, colorless amorphous **8** was isolated and recrystallized from i-PrOH: colorless needles (725 mg, 40%). M.p. 125–128°. TLC (*B*): R_f 0.3. UV (MeOH): 233 (55600), 272 (4200), 283 (4300), 305 (6500). ^{1}H-NMR ((D$_6$)DMSO): 2.37, 2.40 (2*s*, 2 arom. Me); 2.70 (*m*, H–C(2′)); 3.21 (*m*, H–C(2′)); 4.46 (*m*, H–C(4′), 2 H–C(5′)); 5.80 (*m*, H–C(3′)); 6.60 (‘*t*’, *J* = 6.2, H–C(1′)); 7.33–7.90 (4*d*, *J* = 8.1, 8 arom. H); 7.44 (*s*, NH_2); 8.11 (*s*, H–C(3)). Anal. calc. for $C_{26}H_{24}ClN_5O_5$ (521.96): C 59.83, H 4.63, Cl 6.79, N 13.42; found: C 59.87, H 4.65, Cl 6.68, N 13.36.

From the second zone, yellowish amorphous **9** was isolated and recrystallized from MeOH: pale yellow needles (715 mg, 39%). M.p. 141°. TLC (*C*): R_f 0.3. UV (MeOH): 230 (41700), 278 (7900), 327 (4900). ^{1}H-NMR ((D$_6$)DMSO): 2.37, 2.40 (2*s*, 2 arom. Me); 2.78 (*m*, H–C(2′)); 3.05 (*m*, H–C(2′)); 4.44 (*m*, H–C(4′)); 4.57 (*m*, 2 H–C(5′)); 5.80 (*m*, H–C(3′)); 6.41 (‘*t*’, *J* = 5.7, H–C(1′)); 7.33–7.90 (4*d*, *J* = 8.1, 8 arom. H); 8.31 (*s*, NH_2); 8.79 (*s*, H–C(3)). Anal. calc. for $C_{26}H_{24}ClN_5O_5$ (521.96): C 59.83, H 4.63, Cl 6.79, N 13.42; found: C 59.97, H 4.81, Cl 6.63, N 13.25.

*1-(2-Deoxy-β-*D*-*erythro*-pentofuranosyl)-1*H*-pyrazolo[3,4-*d*]pyrimidin-6-amine* (**2**). To a soln. of **8** (1.25 g, 2.39 mmol) in THF (120 ml), 10% Pd/C (0.5 g) and Et_3N (1 ml) were added, and the mixture was hydrogenated for 3 h at r.t. The soln. was filtered and the catalyst washed with hot MeOH/THF. The combined filtrate was evaporated and the residue dissolved in 0.5M NaOMe/MeOH (16 ml) and stirred for 1 h at r.t. Column chromatography (*D*) yielded **1** as an amorphous solid, which was crystallized from H_2O: colorless needles (410 mg, 68%). M.p. 147–149°. TLC (*E*): R_f 0.6. UV (MeOH): 229 (25500), 305 (5900). ^{1}H-NMR ((D$_6$)DMSO): 2.19 (*m*, H–C(2′)); 2.77 (*m*, H–C(2′)); 3.42 (*m*, 2 H–C(5′)); 3.77 (*m*, H–C(4′)); 4.41

(*m*, H–C(3′)); 4.72 (*t*, *J* = 5.6, OH–C(5′)); 5.24 (*d*, *J* = 4.2, OH–C(3′)); 6.46 (‘*t*’, *J* = 6.5, H–C(1′)); 6.95 (*s*, NH_2); 8.00 (*s*, H–C(3)); 8.80 (*s*, H–C(4)). Anal. calc. for $C_{10}H_{13}N_5O_3$ (251.24): C 47.81, H 5.22, N 27.87; found: C 47.89, H 5.35, N 27.73.

*2-(2-Deoxy-β-*D-erythro-*pentofuranosyl)-1*H-*pyrazolo[3,4-*d*]pyrimidin-6-amine* (**10**). As described for **2**, with **9** (1.2 g, 2.3 mmol), 10% Pd/C (350 mg) and Et_3N (2 ml) in THF (200 ml) (8 h). Crystallization from i-PrOH yielded **10** (250 mg, 43%). Colorless needles. M.p. 176–177°. TLC (*E*): R_f 0.3. UV (MeOH): 222 (20300), 284 (6800), 318 (4300). ^{1}H-NMR ((D$_6$)DMSO): 2.33 (*m*, H–C(2′)); 2.59 (*m*, H–C(2′)); 3.56 (*m*, 2 H–C(5′)); 3.90 (*m*, H–C(4′)); 4.41 (*m*, H–C(3′)); 5.05 (*t*, *J* = 5.6, OH–C(6′)); 5.34 (*d*, *J* = 4.3, OH–C(3′)); 6.24 (‘*t*’, *J* = 5.9, H–C(1′)); 6.61 (*s*, NH_2); 8.52 (*s*, H–C(3)); 9.00 (*s*, H–C(4)). Anal. calc. for $C_{10}H_{13}N_5O_3$ (251.24): C 47.81, H 5.22, N 27.87; found: C 47.99, H 5.26, N 27.80.

*1-(2-Deoxy-β-*D-erythro-*pentofuranosyl)-*N-*[(dimethylamino)methylidene]-1*H-*pyrazolo[3,4-*d*]pyrimidin-6-amine* (**12a**). A soln. of **2** (360 mg, 1.43 mmol) in DMF (1.5 ml) was treated with dimethylformamide dimethyl acetal (3 ml), and the mixture was stirred at r.t. for 2 h. The solvent was evaporated with toluene and acetone (2 × 20 ml) to yield a colorless foam. The product was purified by FC (*D*): **12a** (320 mg, 73%). TLC (*D*): R_f 0.3. UV (MeOH): 228 (15200), 262 (29000), 312 (25500). ^{1}H-NMR ((D$_6$)DMSO): 2.24 (*m*, H–C(2′)); 2.77 (*m*, H–C(2′)); 3.08 (*s*, MeN); 3.15 (*s*, MeN); 3.47 (*m*, 2 H–C(5′)); 3.81 (*m*, H–C(4′)); 4.43 (*m*, H–C(3′)); 4.76 (*t*, *J* = 5.6, OH–C(5′)); 5.28 (*d*, *J* = 4.3, OH–C(3′)); 6.61 (‘*t*’, *J* = 6.3, H–C(1′)); 8.15 (*s*, H–C(3)); 8.76 (*s*, H–C(4)); 8.99 (*s*, CH=N). Anal. calc. for $C_{13}H_{18}N_6O_3$ (306.3): C 50.97, H 5.92, N 27.44; found: C 51.01, H 5.89, N 27.43.

N-*[1-(2-Deoxy-β-*D-erythro-*pentofuranosyl)-1*H-*pyrazolo[3,4-*d*]pyrimidin-6-yl]-2-phenoxyacetamide* (**12b**). Compound **2** (150 mg, 0.6 mmol) was dried by co-evaporation with pyridine. The residue was dissolved in pyridine (3 ml) and Me_3SiCl (390 µl, 3 mmol) was added. After stirring for 10 min, 2,4,5-trichlorophenyl phenoxyacetate (0.6 g, 1.8 mmol) in pyridine (5 ml) was added, and the mixture was kept at 40° for 12 h. Then, the mixture was cooled with an ice bath and H_2O (500 µl) was added. After 5 min, conc. aq. ammonia (0.5 ml) was added, the mixture evaporated, and the product purified by FC (*D*): **12b** (100 mg, 43%). Colorless foam. UV (MeOH): 233 (29800), 277 (9500), 282 (9300). ^{1}H-NMR ((D$_6$)DMSO): 2.30 (*m*, H–C(2′)); 2.84 (*m*, H–C(2′)); 3.48 (*m*, 2 H–C(5′)); 3.82 (*m*, H–C(4′)); 4.49 (*m*, H–C(3′)); 4.70 (*t*, *J* = 5.7, OH–C(5′)); 5.08 (*d*, *J* = 3.5, PhOCH_2); 5.31 (*d*, *J* = 4.4, OH–C(3′)); 6.62 (‘*t*’, *J* = 6.4, H–C(1′)); 6.92–7.32 (*m*, 5 arom. H); 8.33 (*s*, H–C(3)); 9.18 (*s*, H–C(4)); 10.99 (*s*, NH). Anal. calc. for $C_{18}H_{19}N_5O_5$ (385.37): C 56.10, H 4.97, N 18.17; found: C 56.32, H 4.80, N 17.98.

N-*[1-(2-Deoxy-β-*D-erythro-*pentofuranosyl)-1*H-*pyrazolo[3,4-*d*]pyrimidin-6-yl]formamide* (**12c**). Compound **13** (200 mg, 0.34 mmol) was treated with Cl_3CCOOH (3 ml), for 5 min. Then, the precipitate was filtered off and washed with CH_2Cl_2: **12c** (69 mg, 73%). TLC (*D*): R_f 0.3. UV (MeOH): 230 (37500), 287 (14100). ^{1}H-NMR ((D$_6$)DMSO): 2.31 (*m*, H–C(2′)); 2.84 (*m*, H–C(2′)); 3.51 (*m*, 2 H–C(5′)); 3.85 (*m*, H–C(4′)); 4.47 (*m*, H–C(3′)); 4.68 (*t*, *J* = 5.6, OH–C(5′)); 5.29 (*d*, *J* = 4.3, OH–C(3′)); 6.60 (‘*t*’, *J* = 6.4, H–C(1′)); 8.32 (*s*, H–C(3)); 9.14 (*s*, H–C(4)); 9.51 (*d*, *J* = 9.4, NH); 10.82 (*d*, *J* = 9.5, H–C=O). Anal. calc. for $C_{11}H_{13}N_5O_4$ (279.25): C 47.31, H 4.69, N 25.08; found: C 47.27, H 4.62, N 24.78.

N-*{1-[2-Deoxy-*5-O-*(4,4′-dimethoxytrityl)-β-*D-erythro-*pentofuranosyl]-1*H-*pyrazolo[3,4-*d*]pyrimidin-6-yl}-formamide* (**13**). Compound **12a** (221 mg, 0.72 mmol) was dried by repeated co-evaporation with anh. pyridine and suspended in dry pyridine (2 ml). The soln. was stirred in the presence of 4-(dimethylamino)pyridine (10 mg, 0.08 mmol) and 4,4′-dimethoxytriphenylmethyl chloride (315 mg, 0.93 mmol) for 4 h. The mixture was diluted with 5% aq. $NaHCO_3$ soln. (20 ml) and extracted with CH_2Cl_2 (3 × 20 ml). The combined org. layer was dried (Na_2SO_4) and evaporated, and the product purified by FC (*F*): **13** (306 mg, 73%). Colorless foam. TLC (*F*): R_f 0.3. UV (MeOH): 235 (32000), 283 (10000). ^{1}H-NMR ((D$_6$)DMSO): 2.31 (*m*, H–C(2′)); 2.81 (*m*, H–C(2′)); 3.05 (*m*, 2 H–C(5′)); 3.69 (2*s*, 2 MeO); 3.94 (*m*, H–C(4′)); 4.55 (*m*, H–C(3′)); 5.36 (*d*, *J* = 4.8, OH–C(3′)); 6.62 (‘*t*’, *J* = 4.7, H–C(1′)); 6.69–7.8 (*m*, 13 arom. H); 8.26 (*s*, H–C(3)); 9.13 (*s*, H–C(4)); 9.50 (*d*, *J* = 9.4, NH); 11.23 (*d*, *J* = 9.5, H–C=O). Anal. calc. for $C_{32}H_{31}N_5O_6$ (581.64): C 66.05, H 5.37, N 12.04; found: C 65.77, H 5.45, N 11.85.

N-*{1-[2-Deoxy-*5-O-*(4,4′-dimethoxytrityl)-β-*D-erythro-*pentofuranosyl]-1*H-*pyrazolo[3,4-*d*]pyrimidin-6-yl}formamide (2-Cyanoethyl Diisopropylphosphoramidite)* (**14**). To a soln. of **13** (250 mg, 0.43 mmol) and (i-Pr)$_2$EtN (143 µl, 0.86 mmol) in anh. THF (2 ml), 2-cyanoethyl diisopropylphosphoramidochloridite (120 µl, 0.52 mmol) was added at r.t. After 30 min, the mixture was diluted with CH_2Cl_2 (20 ml) and quenched with 5% $NaHCO_3$ soln. (20 ml). Then the aq. layer was extracted with CH_2Cl_2 (3 × 20 ml), the combined org. layer dried (Na_2SO_4) and evaporated, and the colorless foam applied to FC (column 2 × 10 cm, *G*): **14** (242 mg, 72%). TLC (*E*): R_f 0.9. ^{31}P-NMR ($CDCl_3$): 149.85, 149.91.

REFERENCES

[1] M. F. Goodman, *Proc. Natl. Acad. Sci. U.S.A.* **1997**, *94*, 10493.
[2] S. M. Watanabe, M. F. Goodman, *Proc. Natl. Acad. Sci. U.S.A.* **1981**, *78*, 2864.
[3] T. M. Jovin, in 'Nucleic Acids and Molecular Biology', Eds. F. Eckstein and D. M. J. Lilley, Springer Verlag, Berlin-Heidelberg, 1991; Vol. 5, p. 25.
[4] A. Ronen, *Mutat. Res.* **1979**, *75*, 1.
[5] E. Fresse, *Proc. Natl. Acad. Sci. U.S.A.* **1959**, *45*, 622.
[6] D. C. Ward, E. Reich, L. Stryer, *J. Biol. Chem.* **1969**, *244*, 1228.
[7] B. Holz, S. Klimasauskas, S. Serva, E. Weinhold, *Nucleic Acids Res.* **1998**, *26*, 1076.
[8] B. W. Allan, N. O. Reich, J. M. Beecham, *Biochemistry* **1999**, *38*, 5308.
[9] D. Xu, K. O. Evans, T. M. Nordlund, *Biochemistry* **1994**, *33*, 9592.
[10] R. A. Hochstrasser, T. E. Carver, L. C. Sowers, D. P. Millar, *Biochemistry* **1994**, *33*, 11971.
[11] T. M. Nordlund, S. Andersson, L. Rigler, A. Gräslund, L. W. McLaughlin, *Biochemistry* **1989**, *28*, 9095.
[12] R. A. Hochstrasser, T. E. Carver, L. C. Sowers, D. P. Millar, *Biochemistry* **1994**, *33*, 11971.
[13] J. J. Fox, I. Wempen, A. Hampton, I. L. Doer, *J. Am. Chem. Soc.* **1958**, *80*, 1669.
[14] P. P. Kung, R. A. Jones, *Tetrahedron Lett.* **1991**, *32*, 3919.
[15] A. Stimac, D. Muhic, J. Kobe, *Nucleosides Nucleotides* **1994**, *13*, 625.
[16] R. Eritja, B. E. Kaplan, D. Mhaskar, L. C. Sowers, J. Petruska, M. F. Goodman, *Nucleic Acids Res.* **1986**, *14*, 5869.
[17] L. W. McLaughlin, T. Leong, F. Benseler, N. Piel, *Nucleic Acids Res.* **1988**, *16*, 5631.
[18] J. Fujimoto, Z. Nuesca, M. Mazurek, L. C. Sowers, *Nucleic Acids Res.* **1996**, *24*, 754.
[19] S. Schmidt, D. Cech, *Nucleosides Nucleotides* **1995**, *14*, 1445.
[20] F. Seela, U. Engelke, *Liebigs Ann. Chem.* **1985**, 1175.
[21] F. Seela, G. Becher, *Collect. Czech. Chem. Commun. (Symposium Series)* **1999**, 320.
[22] F. Seela, C. Wei, G. Becher, M. Zulauf, P. Leonard, *Bioorg. Med. Chem. Lett.*, in press.
[23] F. Seela, H. Steker, *Helv. Chim. Acta* **1986**, *69*, 1602.
[24] H. Steker, Dissertation, Universität – Gesamthochschule Paderborn, 1988.
[25] P. Nuhn, A. Zschunke, D. Heller, G. Wagner, *Tetrahedron* **1969**, *25*, 2139.
[26] B. C. Froehler, M. D. Maetteucci, *Nucleic Acids Res.* **1983**, *11*, 8031.
[27] J. Zemlicka, A. Holy, *Collect. Czech. Chem. Commun.* **1967**, *32*, 3159.
[28] D. P. C. McGee, J. C. Martin, A. S. Webb, *Synthesis* **1983**, 540.
[29] A. Cano, M. F. Goodman, R. Eritja, *Nucleosides Nucleotides* **1994**, *13*, 501.
[30] H. Schaller, G. Weimann, B. Lerch, H. G. Khorana, *J. Am. Chem. Soc.* **1963**, *85*, 3821.
[31] F. Seela, A. Melenewski, *Eur. J. Org. Chem.* **1999**, 485.
[32] F. Seela, G. Becher, unpublished results.
[33] B. C. Froehler, 'Protocols for Oligonucleotides and Analogs', in 'Methods in Molecular Biology', Ed. E. S. Agrawal, Humana Press, Totowa, N. J., 1993, Vol. 20, p. 63.
[34] F. Seela, W. Bussmann, *Nucleosides Nucleotides* **1985**, *4*, 3391.
[35] F. Seela, M. Zulauf, *J. Chem. Soc., Perkin Trans. 1* **1999**, 479.
[36] C. A. Brennan, R. I. Gumport, *Nucleic Acids Res.* **1985**, *13*, 8665.
[37] K. H. Scheit, H. R. Rackwitz, *Nucleic Acids Res.* **1982**, *10*, 4059.
[38] L. C. Sowers, G. V. Fazakerley, R. Eritja, B. E. Kaplan, M. F. Goodman, *Proc. Natl. Acad. Sci. U.S.A.* **1986**, *83*, 5434.
[39] P. A. Fagan, C. Fàbrega, R. Eritja, M. F. Goodman, D. E. Wemmer, *Biochemistry* **1996**, *35*, 4026.
[40] F. Seela, C. Wei, *Helv. Chim. Acta* **1999**, *82*, 726.
[41] F. Seela, G. Becher, H. Rosemeyer, H. Reuter, G. Kastner, I. Mikhailopulo, *Helv. Chim. Acta* **1999**, *82*, 105.
[42] T. M. Nordlund, S. Andersson, L. Nilsson, R. Rigler, A. Gräslund, L. W. McLaughlin, *Biochemistry* **1989**, *28*, 9095.
[43] T. Ha, T. Enderle, D. F. Ogletree, D. S. Chemila, P. R. Selvin, S. Weiss, *Proc. Natl. Acad. Sci. U.S.A.* **1996**, *93*, 6264.

Received January 28, 2000